Thuraya Y. Sabri
Awatif S. Jasim

Department of Physics,
College of Science,
University of Tikrit,
Tikrit, IRAQ

Effect of MWCNT Concentration on Characteristics of Bi_2O_3/MWCNT Nanocomposite Films Prepared by Pulsed-Laser Deposition

In this paper, pure Bi_2O_3 and Bi_2O_3/MWCNT thin films were prepared with concentrations of MWCNT in the ratios of 0.5, 1, and 2 wt.% by the pulsed-laser deposition (PLD) method on glass substrates to characterize and analyze their topography, morphology and optical properties. It was shown that all prepared films have a polycrystalline nature with tetragonal *β*-Bi_2O_3 structure. The grain size increases with increasing MWCNT concentration. The absorbance of the prepared films was found to increase with increasing MWCNT concentration, but the band gap values decrease from 2.8 to 2.0 eV.

***Keywords*:** Carbon nanotubes; Nanocomposite films; β-Bi_2O_3; Pulsed-laser deposition
Received: 28 October 2024; **Revised:** 12 December; **Accepted:** 19 December 2024

1. Introduction

Among semiconducting photosensitive materials are bismuth oxide thin films. They have a high refractive index and a large energy band gap, making them useful for different applications such as optical coatings, solar cells, integrated circuits, and gas sensors [1-3]. This material has five polymorphs of Bi_2O_3, known as α-Bi_2O_3, β-Bi_2O_3, γ-Bi_2O_3, δ-Bi_2O_3, and ω-Bi_2O_3, which were reported, each one having different crystal structures and different electrical, optical, and mechanical properties, as the β-phase has a tetragonal structure; it is an n-type semiconductor and has an approximate band gap of 2.58 eV [4-6].

The overall oxides mixtures composition depends on conditions and preparation techniques, such as the type, nature, and temperature of the substrate at the deposition of the oxide [7]. Structural, chemical, and electrical properties of a material are dependent on its method of synthesis [8]. Several techniques were employed to prepare Bi_2O_3 thin films, including chemical bath deposition [9], chemical spray pyrolysis [10], sol-gel [11], thermal oxidation of vacuum evaporated [12], etc. Pulsed laser deposition is a method that is used to prepare Bi_2O_3 thin films in this work.

Carbon nanotubes (CNTs) have different applications because it has exceptional properties, such as good electrical and thermal conductivity, good mechanical properties, photon absorbers working on enhanced spectral absorption areas, and providing a path for electron conduction when used with semiconductor oxides. CNT-based nanocomposites have shown better applications in nano-electronics and energy storage devices [13]. To form good composite material with nanostructure properties, most metal oxides with carbon nanotubes (CNTs), such as ZnO [14], CuO [15], and TiO_2 [16]. CNT structures have unique properties with a diameter ranging from one to a few nanometers as compared to non-nano homologs. They have two forms: single-walled carbon nanotubes (SWCNT) and multi-walled carbon nanotubes (MWCNT). SWCNT are single graphene rolls with diameters of 0.8 to a few nanometers, while MWCNT are concentric graphene tubes that can have diameters from a few to more than a hundred nanometers [17,18]. More recently, used a different form of MWCNT as a CNT for reinforcement [19]. MWCNT are the most ideal CNT candidates among the different CNT types to be incorporated into the polymer matrix [20]. Figure (1) shows pictographs and field-emission scanning electron microscope (FE-SEM) images of SWCNT and MWCNT [21].

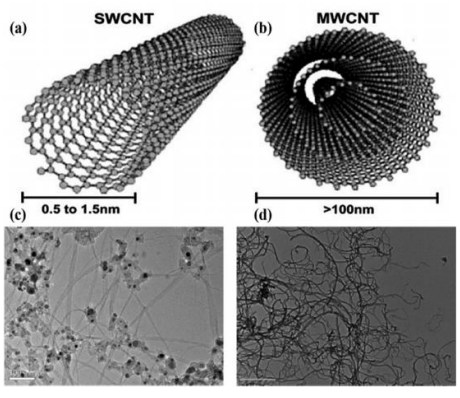

Fig. (1) Pictorial graph of (a) SWCNT and (b) MWCNT and SEM image of (c) SWCNT and (d) MWCNT [21]

2. Experimental Part

Bi_2O_3 nanopowder with purity of 99.9% has been used as a matrix material with a weight of 2 g, and the MWCNT was used as a dopant for preparing Bi_2O_3/MWCNT thin films with MWCNT concentrations of 0.5, 1, and 2 wt.%, which were blended and pressed using a hydraulic press of 5 tons

for 10 minutes to obtain circular discs with a diameter of 2 cm and a thickness of 0.3 cm. Glass substrates with dimensions of 75×25×1.2 mm have been cleaned with acetone in an ultrasonic bath and then washed again with ethanol. Bi_2O_3 thin films and Bi_2O_3/MWCNT films were prepared by the pulsed-laser deposition (PLD) technique. The glass substrates were placed, after being cleaned, on a holder in front of the target surface; the distance between the substrate and the target was 2.5 cm. The laser beam has been focused on the target at the angle of 45° inside the deposition chamber. An Nd:YAG laser with 1064 nm wavelength, 6 Hz frequency, and 400 mJ energy was sued for the PLD at a number of pulses of 300 pulses at room temperature. The process was depositing thin films under vacuum (10^{-3} Torr). All the prepared films were annealed at 400°C for 1 hour. Figure (2) shows a scheme of the PLD system. To characterize the prepared thin films, x-ray diffraction (XRD), field-emission scanning electron microscopy (FE-SEM), and atomic force microscopy (AFM) were employed. The absorption spectra of the films were measured using a UV-Visible spectrophotometer in the wavelength range of 300-1100 nm.

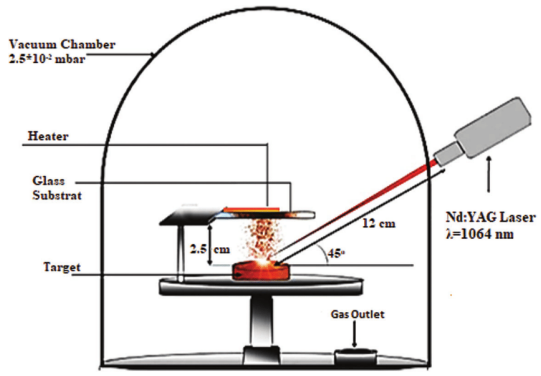

Fig. (2) Technique for experimental representation of PLD

3. Results and Discussion

The important purpose in this part is to know the type of crystalline structure of the semiconducting materials used in this study. Figure (3) shows the XRD patterns for pure Bi_2O_3 and Bi_2O_3/MWCNT thin films with different MWCNT concentrations (0.5, 1, and 2 wt.%) deposited on glass substrates by the PLD technique. It shows a polycrystalline structure for all films with a tetragonal β-Bi_2O_3 structure. The crystal planes (201), (220), (222), (421), and (402) indicate the Bi_2O_3 phase with preferred orientation at $2\theta = 27.9°$ in the (201) plane; as shown in table (1). These results are in agreement with the standard JCPDS card no. 00-027-0050 of the Bi_2O_3.

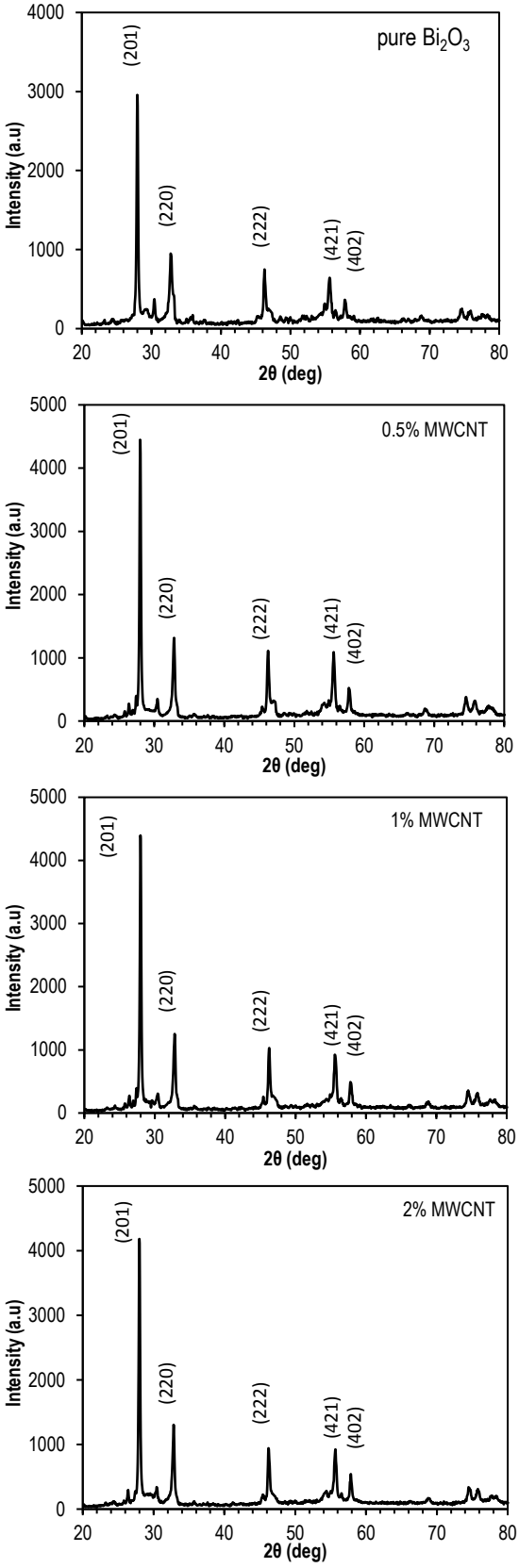

Fig. (3) XRD patterns for pure Bi_2O_3 and Bi_2O_3/MWCNT thin films

In addition, no distinct diffraction peaks corresponding to MWCNT nanocomposite at $2\theta \approx 26°$, 45°, and 54° were observed due to the low ratio concentration of MWCNT in prepared films. These results are found to be in good agreement with other research works [22,23]. Also, it was observed that the FWHM of diffraction peaks decreased and the particle size increased with increasing concentration ratio of MWCNT.

Table (1) X-ray parameters for pure Bi_2O_3 and Bi_2O_3/MWCNT thin films

Sample	2θ (deg)	FWHM (deg)	d_{hkl} (Å)	Grain size (nm)	hkl
Pure Bi_2O_3	27.9905	0.2362	3.18778	34.7	(201)
	32.8109	0.2952	2.72963	28.1	(220)
	46.2484	0.2362	1.96304	33.6	(222)
	55.5975	0.3542	1.65307	25.4	(421)
	57.8498	0.2952	1.59395	30.7	(402)
0.5 wt.% MWCNT	27.9898	0.2362	3.18786	34.7	(201)
	32.8272	0.2952	2.72831	28.1	(220)
	46.2323	0.2952	1.96369	29.3	(222)
	55.6308	0.3542	1.65216	25.4	(421)
	57.8472	0.2952	1.59402	30.7	(402)
1 wt.% MWCNT	27.9898	0.2362	3.18786	34.7	(201)
	32.8345	0.2952	2.72772	28.1	(220)
	46.2482	0.2952	1.96305	26.3	(222)
	55.6727	0.2952	1.65101	30.4	(421)
	57.8350	0.3542	1.59433	25.6	(402)
2 wt.% MWCNT	27.9965	0.1771	3.18711	46.2	(201)
	32.841	0.2362	2.72716	35.1	(220)
	46.2358	0.2362	1.96355	36.6	(222)
	55.6388	0.2952	1.65194	30.4	(421)
	57.8285	0.2362	1.59449	38.4	(402)

One of the preferred methods of analyzing the layers of the outer surface of prepared films is atomic force microscopy (AFM). Figure (4) shows 2D AFM images of pure Bi_2O_3 and Bi_2O_3/MWCNT thin films with different concentrations of MWCNT (0.5, 1, and 2 wt.%). It was observed that the surface roughness and average grain size values increased with increasing MWCNT concentration ratio, as shown in table (2). As the surface roughness increases, it has an important benefit in solar cell applications through increasing the angles of radiation falling on the film surface and lowering the reflectivity, therefore, the absorption of the electromagnetic radiation will increase cell efficiency [24].

Table (2) AFM parameters for pure Bi_2O_3 and Bi_2O_3/MWCNT thin films

Simple	Average Roughness (nm)	Roughness (R.M.S.) (nm)	Average Diameter (nm)
Pure Bi_2O_3	59.38	67.53	85.31
0.5 wt.% MWCNT	194.8	223.9	90.24
1 wt.% MWCNT	223.6	274.8	95.14
2 wt.% MWCNT	228.0	284.6	82.55

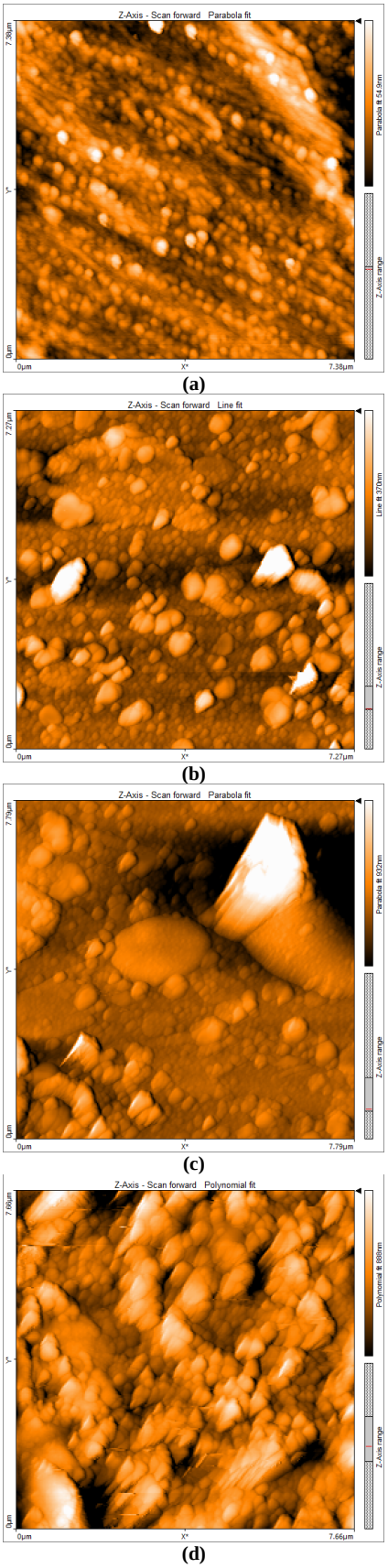

Fig. (4) 2D AFM images for (a) Bi_2O_3 pure, (b) and 0.5 wt.% MWCNT, (c) 1 wt.% MWCNT, and (d) 2 wt.% MWCNT

Figure (5) shows FE-SEM images of pure Bi_2O_3 and Bi_2O_3/MWCNT thin films with different MWCNT concentration (0.5, 1, and 2 wt.%). These micrographs showed a rough microstructure; Bi_2O_3 and MWCNT nanoparticles are in good contact with each other and attached to the substrate. In addition to the morphological structure, the porosity of all films can be observed, and as the MWCNT concentration ratio increases, the porosity of the films becomes larger, whereas Bi_2O_3 nanoparticles become smaller [23].

The measurements of absorption spectra of the prepared films in the wavelength range of 300-1100 nm have been carried out using a UV-visible spectrophotometer and figure (6) shows these spectra for the pure Bi_2O_3 and Bi_2O_3/MWCNT thin films with different MWCNT concentrations (0.5, 1, and 2 wt.%). The highest absorbance of the prepared films is in the visible region (short wavelengths) and then begins to decrease with increasing wavelength. This can be attributed to the fact that the photon energy is not enough to transfer the electron from the valence to the conduction band because the energies of the incident photons are lower than the value of the energy gap. In addition, the absorbance increases with increasing MWCNT concentration.

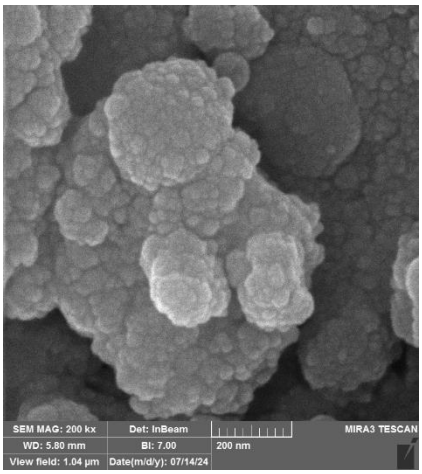

(a)

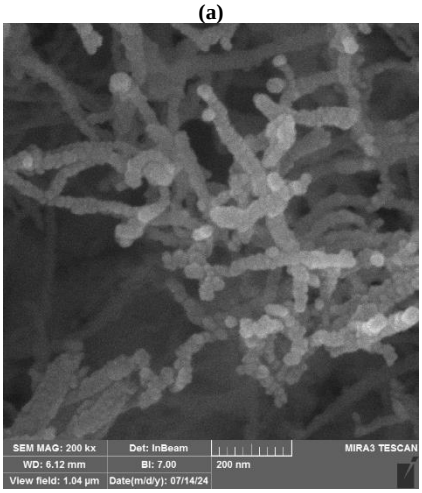

(b)

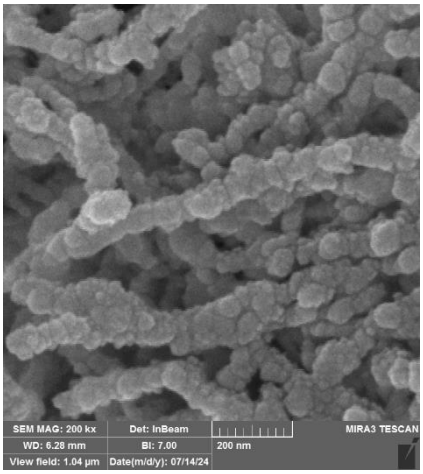

(c)

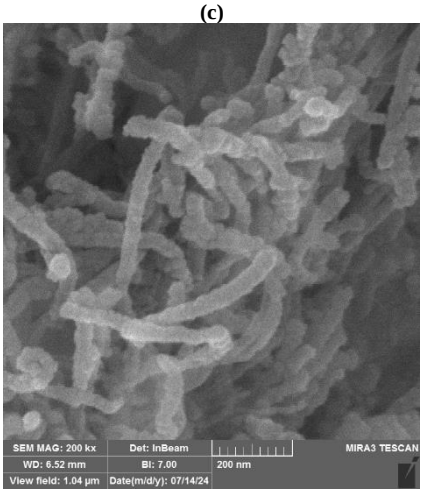

(d)

Fig. (5) FE-SEM images for (a) Bi_2O_3 pure, (b) and 0.5 wt.% MWCNT, (c) 1 wt.% MWCNT, and (d) 2 wt.% MWCNT

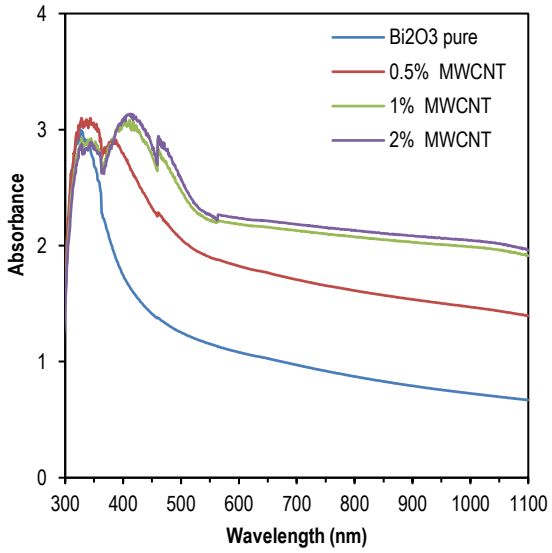

Fig. (6) Absorption spectra of pure Bi_2O_3 and Bi_2O_3/MWCNT thin films

Figure (7) shows that the optical energy gap (E_g) value gradually decreases with increasing MWCNT

concentration for all samples. This decrease in the energy gap may be due to the increase in the density of states that lead to the formation of energy sub-levels within the energy gap.

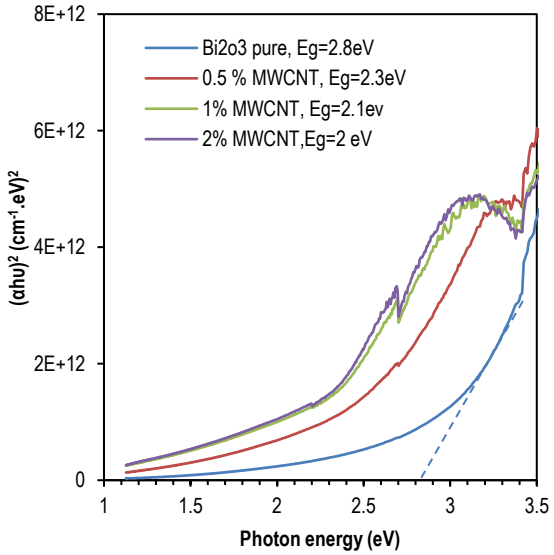

Fig. (7) Energy gap of pure Bi_2O_3 and Bi_2O_3/MWCNT thin films

4. Conclusion

According to the results obtained from this work, it can concluded that all pure Bi_2O_3 and Bi_2O_3/MWCNT thin films with different MWCNT concentrations were successfully produced. These films showed polycrystalline structure with tetragonal β-Bi_2O_3 structure. The surface roughness and average grain size of the prepared films have increased with increasing MWCNT concentration. The MWCNT and Bi_2O_3 nanoparticles are in good contact. The energy gap for the films decreased from 2.8 to 2.0 eV with increasing MWCNT concentration ratio.

References

[1] F. Qin et al., "Template-Free Fabrication of Bi_2O_3 and $(BiO)_2CO_3$ Nanotubes and Their Application in Water Treatment", *Chem. Euro. J.*, 18(51) (2012) 16491-16497.

[2] J. Morasch et al., "Reactively magnetron sputtered Bi_2O_3 thin films: Analysis of structure, optoelectronic, interface, and photovoltaic properties", *phys. stat. sol. a*, 211(10) (2014) 93-100.

[3] F. Tudorache et al., "Humidity sensors applicative characteristics of granularized and porous Bi_2O_3 thin films prepared by oxygen plasma-assisted pulsed laser deposition", *Superlatt. Microstruc.*, 77 (2015) 276-285.

[4] H.T. Fan et al., "δ-Bi_2O_3 thin films prepared by reactive sputtering: Fabrication and characterization", *Thin Solid Films*, 513 (2006) 142-147.

[5] S. Park et al., "Enhanced Gas Sensing Properties of Bi_2O_3-Core/In_2O_3-Shell Nanorod Gas Sensors", *Bull. Korean Chem. Soc.*, 33(10) (2012) 3368-3372.

[6] A.J. Salazar-Pérez et al., "Structural evolution of Bi_2O_3 prepared by thermal oxidation of bismuth nanoparticles", *Superficies y Vacío*, 18(3) (2005) 4-8.

[7] S. Condurache-Bota et al., "Optical and electrical properties of thermally oxidized bismuth thin films", *Appl. Surf. Sci.*, 257(24) (2011)10545-10550.

[8] L. Leontie et al., "Structural and optical characteristics of bismuth oxide thin films", *Surf Sci.*, 507-510 (2002) 480-485.

[9] T.P. Gujar et al., "Bismuth oxide thin films prepared by chemical bath deposition (CBD) method: annealing effect", *Appl. Surf. Sci.*, 250(1-4) (2005) 161-167.

[10] V.V. Killedar, C.H. Bhosale and C.D. Lokhande, "Characterization of Spray Deposited Bismuth Oxide Thin Films from Non-Aqueous Medium", *Turkish J. Phys.*, 22 (1998) 825-830.

[11] M. Gotić, S. Popović and S. Musić, "Influence of synthesis procedure on the morphology of bismuth oxide particles", *Mater. Lett.*, 61(3) (2007) 709-714.

[12] S. Patil and V. Puri, "Electromagnetic properties of bismuth oxide thin film deposited on glass and alumina", *Arch. Appl. Sci. Res.*, 3(2) (2011) 14-24.

[13] M. Scarselli, P. Castrucci and M. De Crescenzi, "Electronic and optoelectronic nano-devices based on carbon nanotubes", *J. Phys. Cond. Matter*, 24(31) (2012) 313202.

[14] G.Q. Mo, J. Ye and W.D. Zhang, "Unusual electrochemical response of ZnO nanowires-decorated multiwalled carbon nanotubes", *Electrochimica Acta*, 55(2) (2009) 511-515.

[15] J. Zheng et al., "Nanocomposites of Carbon Nanotube (CNTs)/CuO with High Sensitivity to Organic Volatiles at Room Temperature", *Procedia Eng.*, 36 (2012) 235–245.

[16] S. Da Dalt, A.K. Alves and C.P. Bergmann, "Preparation and Performance of TiO_2-ZnO/CNT Hetero-Nanostructures Applied to Photodegradation of Organic Dye", *Mater. Res.*, 19(6) (2016) 1372–1375.

[17] Q. Zhao, Z. Gan and Q. Zhuang, "Electrochemical Sensors Based on Carbon Nanotubes", *Electroanal.*, 14(23) (2002) 1609-1613.

[18] K. Balasubramanian and M. Burghard, "Chemically Functionalized Carbon Nanotubes", *Small*, 1(2) (2005) 180-192.

[19] M. Paszkiewicz et al., "Helical Multi-walled Carbon Nanotubes as an Efficient Material for the Dispersive Solid-Phase Extraction of Low and High Molecular Weight Polycyclic Aromatic

Hydrocarbons from Water Samples: Theoretical Study", *Water Air Soil Pollut*., 229:253 (2018) 1-15.

[20] S.M. Rahimian-Koloor, S.M. Hashemianzadeh and M.M. Shokrieh, "Effect of CNT structural defects on the mechanical properties of CNT/Epoxy nanocomposite', *Phys. B: Cond. Matter*, 540 (2018) 16-25.

[21] W. Andreoni (ed.), **"The physics of fullerene-based and fullerene-related material"**, Springer (Netherlands, 2000).

[22] R. Vyas et al., "Synthesis and Hydrogen Sensing Properties of CNT-ZnO nanocomposite thin films", *Int. J. Mod. Phys. Conf. Ser*., 22 (2013) 478-482.

[23] A.S. Abd-Alsada and M.F.A. Ali, "Impact of CNT Concentrations on Structural, Morphological and Optical Properties of ZnO:CNT Nano composite Films", *J. Phys. Conf. Ser*., 2114 (2021) 012020.

[24] R.A. Ahmed et al., "Synthesis and Characterization of $CdO_{1-x}ZnO_x$ for Solar Cell Applications", *Dig. J. Nanomater. Biostruct.*, 14(1) (2019) 15-22.

